JOURNAL OF MATERIALS SCIENCE **33** (1998) 5265–5273

The kinetics of surface induced sinter crystallization and the formation of glass-ceramic materials

I. GUTZOW, R. PASCOVA, A. KARAMANOV
Institute of Physical Chemistry, Bulgarian Academy of Sciences, Sofia 1113, Bulgaria
J. SCHMELZER
Fachbereich Physik, Universität Rostock, D-18051 Rostock, Germany

A thorough analysis is given of a process which is of great importance for the formation of many present day glass ceramic materials: sinter-crystallization. In the first part of the paper the problems determining surface induced nucleation of glasses are analyzed, emphasis being given to the influence of elastic strains and surface contamination by active substrates. The second stage of the analysis is centred on the dependence of crystal growth and overall crystallization kinetics on the mean size of an ensemble of sintering glass grains. Here a formalism is derived, connecting overall crystallization with the mean size of the crystallizing system of glass particles. In the third part the interdependence sintering – crystallization is investigated. Several cases of this interrelation are analyzed in details for different mechanisms of growth of nuclei, athermally formed on the grain surface.

1. Introduction

There are different ways to synthesize glass-ceramic materials, the most commonly used method being the introduction of insoluble crystallization cores into the bulk of the melt. Thus, one of the possible modes of crystallization catalysis – heterogeneous nucleation induced by active substrates is achieved. A survey of possibilities in this respect may be traced in a number of monographs [1–4] as well as in a review article [5], written by one of the present authors.

However, already in the first applications of heterogeneous nucleation catalysis of a glass forming system performed more than two hundred years ago (see the remarkable tractate of M. de Reaumure [6] and its analysis in [5]) another possibility was exploited: the process of surface induced nucleation of glass. To do this Reaumure simply covered the surface of glass articles heat treated in an oven with nucleation cores (e.g. quartz sand etc.) in powdered form.

Further developments and results reported in the earliest reviews and books devoted to glass science (see Tammann [7], Blumberg [8]) revealed another remarkable effect: any free glass surface, seeded or not seeded with foreign crystallization cores is the preferred site for the start of crystallization. Grained glass samples devitrify more easily than bulk glass samples and upon a process of simultaneous amorphous state sintering and crystallization, glass-ceramic materials can be obtained. In present day literature this process is known as sinter-crystallization.

It may be even argued that one of the ancient Egyptian techniques of glass fabrication was in fact a primitive form of a sinter crystallization process: glass was fritted, grained and sinter-crystallized in refractory moulds [9].

The first present day attempt to form glass-ceramic materials by a process of sinter-crystallization was reported 1953 by Sack [10]. Since then a number of applications of this process have been found, especially in producing marble-like materials for architectonic applications (e.g. Neoparies, see [2, 11] cordierite- [12] and diopside- [13] type materials). It turned out that surface induced nucleation and subsequent crystallization can be even more effective than any other method of nucleation catalysis (see the discussion in [4, 14]). Of particular significance in this respect were recent experimental investigations in which detailed information concerning the kinetics of surface nucleation [15–17], the kinetics of overall crystallization of grained glass samples [18] and the process of sintering [19] is given.

The cited investigations showed on one side that sinter crystallization is a process of significant practical importance. On the other side it turned out that this process is also a challenge from a theoretical and experimental point of view. The most significant in this respect is the analysis of the nature and causes of surface catalysis itself.

These investigations revealed also that the kinetics of crystallization and of sintering of grained glass samples is a very interesting problem, the specific features of which were indicated years ago in one of our previous studies [20].

A new direction of technological research connected with sinter-crystallization was found in the possibility

(see [21]) to form by this process glass-ceramics from ecologically important waste materials (fly ashes, urban wastes [22] etc.). Such applications may be of utmost ecological significance as can be seen from an analysis of different possible ways as they are summarized e.g. in [23].

In the present contribution three main problems are under discussion:

(i) the causes of surface induced nucleation,
(ii) the theoretical background for a simple description of the kinetics of surface induced crystallization of an ensemble of glass grains of radius R_o and
(iii) the time dependence of the sintering process of such a crystallizing grained glass sample.

To every one of these three problems one of the following sections is devoted.

In Section 4 the influence of glass relaxation on these processes is also discussed.

In this way, we hope, by the analysis of the main features of the kinetics of sinter-crystallization, a more comprehensive understanding of the process as a whole may be achieved.

2. Surface induced crystallization of glasses

Different hypotheses have been proposed in order to explain the already mentioned fact that as a rule, devitrification of a glass heat treated above its transformation temperature T_g begins from the surface of samples [14]. Formation of active silica gels on the surface (see Tabata's paper [24]) as well as influence of air humidity, influence of hypothetical thin "active" surface layers, surface energy effects and surface contaminations have been considered as being responsible for the surface induced nucleation in the devitrification of glasses (see [8, 14, 24]). The first effect, namely the formation of active silica gels on the surface, is possible only for silicate glasses. In recent investigations, however, surface induced nucleation was also observed in metallic alloy glasses where the first hypothesis cannot be applied. The preferential formation of critical crystalline nuclei on the glass/air interface itself is not to be expected considering (as done in [24]) the contribution of the respective surface energies, only: This is evident accounting for the values of the surface energies σ on the crystal/vapour (or crystal/air) and of the crystal/melt interfaces [14] as they follow from Stefan's Rule [4]. According to this Rule the surface energy σ is proportional to the enthalpy difference ΔH between the phases forming the interface and recalling the simple fact that always $\Delta H_{\text{evaporation}} > \Delta H_{\text{melting}}$, it is obvious that $\sigma_{\text{crystal/air}} > \sigma_{\text{crystal/melt}}$ [4].

According to a new idea formulated by the present authors [14, 25], the nucleating activity of free glass surfaces or of smallest grained glass samples is connected with the reduced elastic energy on the glass surface (or in tiny glass dust particles) when compared with the enormous strains produced at nucleus formation in the bulk of an elastic matrix.

According to a well known formalism (see for example [4]) the steady state rate of nucleation I_{ss} can be expressed in the case of melt crystallization as

$$I_{ss} = A_o(1/\eta)\exp(-\Delta G_c^o/kT) \tag{1}$$

where η is the viscosity of the glass-forming melt, k is Boltzmann's constant, T is the absolute temperature and A_o is a constant.

It is seen that the nucleation rate is mainly determined by the work ΔG_c^o of nucleus formation, i.e. of formation of critical size crystalline clusters

$$\Delta G_c^o = (16\pi/3)\left(\sigma^3 v_c^2 / \Delta\mu_o^2\right). \tag{2}$$

It depends on the value of the specific surface energy, σ, on the nucleus-melt interface, on the molar volume, v_c, of the newly formed crystalline phase and on the thermodynamic driving force of crystallization, $\Delta\mu_o$ (the difference of the chemical potentials melt/crystalline phase).

The (o)-superscript in ΔG_c^o in the above equations indicates that the nucleation process is not accompanied by generation of elastic strains.

At an undercooling $\Delta T = T_m - T$ we can express $\Delta\mu_o$ in a simplest approximation [4] as

$$\Delta\mu_o \cong \Delta S_m \Delta T$$

T_m and ΔS_m denoting the temperature and entropy of melting, respectively.

When the nucleation process takes place in the bulk of an elastic body (i.e. at a distance $z \to \infty$ from its surface), instead of Equation 2 we have to write for the work of nucleus formation (see [4, 14, 25, 26])

$$\Delta G_c(z \to \infty) = (16\pi/3)\sigma^3 v_c^2/(\Delta\mu_o - \Delta\varepsilon(z \to \infty))^2. \tag{2a}$$

The additional term $\Delta\varepsilon(z \to \infty)$ in Equation 2a accounts for the decrease of the thermodynamic driving force $\Delta\mu_o$ caused by the generation of elastic strains upon formation of a crystalline nucleus of radius R_c in the bulk of the glass. This term can be expressed as [4, 14, 25]

$$\Delta\varepsilon(z \to \infty) = \text{ɜ}_o \delta^2 V_c. \tag{3}$$

Here $V_c = (4\pi/3)R_c^3$ is the volume of the crystalline nucleus considered. In the same equation the term

$$\delta = (v_g - v_c)/v_c \tag{4}$$

gives the relative difference in molar volumes of the glass (g) and crystal (c), ɜ$_o$ being a combination of the corresponding elastic constants of the crystalline phase and of the glass matrix [14, 4]. It can be shown [14] that in the case of nuclei formation in the vicinity (at a distance z) or on the glass surface ($z = 0$) (see the

models given with Fig. 1) the work of nucleus formation $\Delta G_c(z)$ becomes

$$\Delta G_c(z) = \Delta G_c(z \to \infty)\Phi(\beta(z), \beta(z \to \infty))g(\Xi). \tag{5}$$

Here $\Phi(\beta(z), \beta(z \to \infty))$ is a complicated function of the distance z from the centre of the nucleus to the free glass surface and of the ratios $\beta(z) = \Delta\varepsilon(z)/\Delta\mu_o$ and $\beta(z \to \infty) = \Delta\varepsilon(z \to \infty)/\Delta\mu_o$.

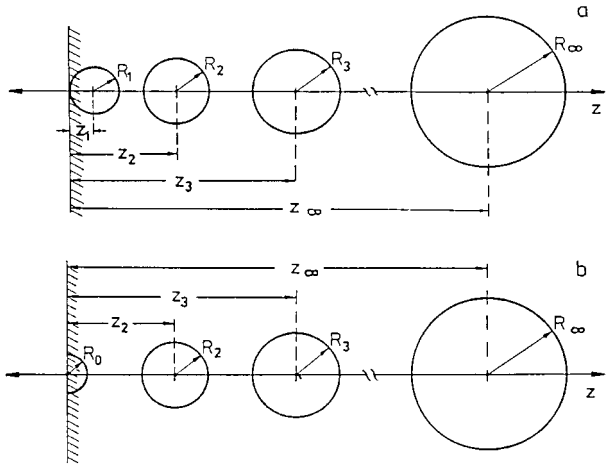

Figure 1 Change of shape and size of critical clusters in dependence on the distance from the free glass surface, z, for two hypothetical models with typical Ξ values: (a) $\Xi = 1$ and (b) $\Xi = 0$. The lowest value of the work of formation of a critical cluster corresponds to a spherical cluster located tangentially to the interface for $\Xi = 1$ (a) and to a hemisphere for $\Xi = 0$ (b).

In Equation 5 the function $g(\Xi)$ is determined by $g(\Xi) = 0.25(1+\Xi)^2(2-\Xi)$ where $\Xi = (\sigma_{vc} - \sigma_{vm})/\sigma_{cm}$ and σ_{vc}, σ_{vm} and σ_{cm}, are the surface energies on the vapour/crystal, vapour/ambient phase and the crystal/ambient phase interfaces, respectively [14, 25].

In Equations 2a and 5 the notations $\Delta G_c(z \to \infty)$ and $\Delta G_c(z)$ show, as already mentioned that the nucleation takes place in the bulk of the glass or at distance z from the free glass surface.

A thorough analysis and the respective derivations are given elsewhere (see [14, 25] and [4]). Here we have to say, only, that the work ΔG_c of critical cluster formation (Equations 2a and 5) was determined considering:

(i) the dependence of ΔG_c on the distance z from the free glass surface
(ii) the dependence of ΔG_c on both σ_{cm} and σ_{vc} when the nucleus is formed directly on the interface.

Fig. 2a illustrates the $\Delta G_c(z)/\Delta G_c(z \to \infty)$ ratio in dependence of the ratio z/R_c for different $\beta(z \to \infty)$ values. It turns out that for all possible values of Ξ formation of critical clusters at the surface of the solid is the more probable the higher the initial value of $\beta(z \to \infty)$, i.e. the greater the difference in molar volumes $(v_g - v_c)$ (cf. Equations 3, 4 and Ref. [4, 14, 25]). Accounting for Stefan's rule, Ξ is nearly equal to 1 for melt crystallization. Thus, elastic strains in combination with the mentioned surface energy values lead to the conclusion that the formation of crystalline clusters is most probable in the immediate vicinity of free surfaces. Similarly, in nucleation in small particles the

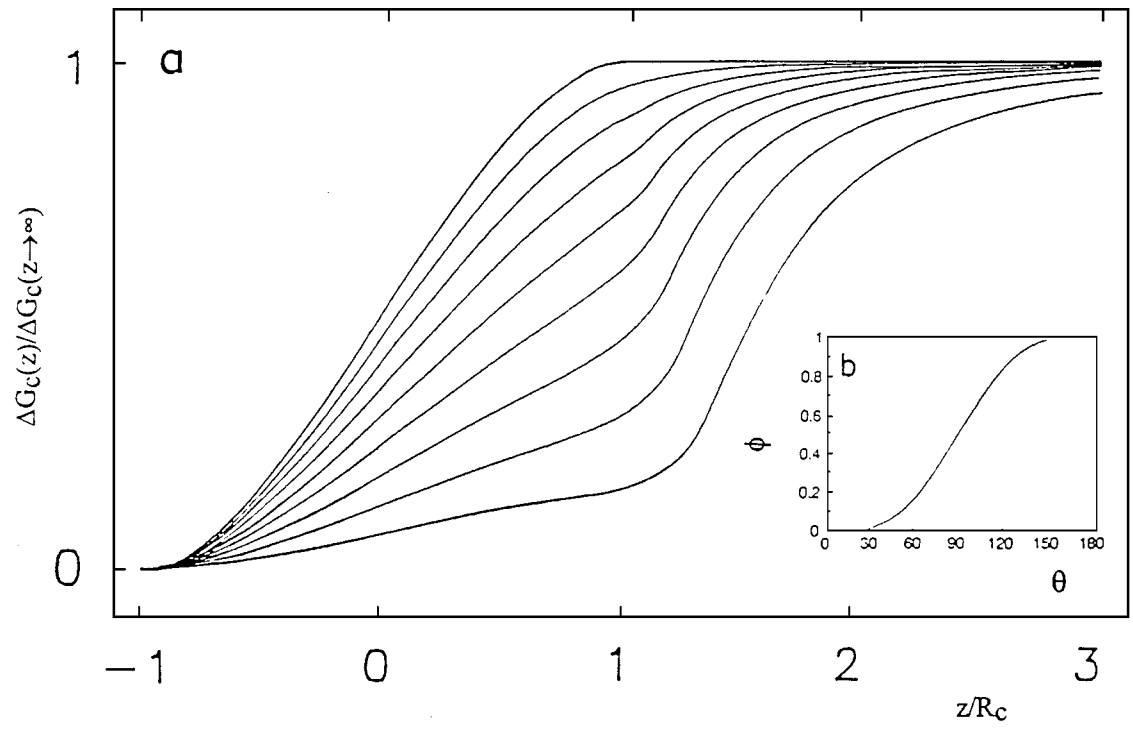

Figure 2 Dependence of the work of nucleation in surface induced crystallization and in heterogeneously catalyzed phase formation. (a) Relative work $\Delta G_c(z)/\Delta G_c(z \to \infty)$ of critical cluster formation in an elastic glass matrix below T_g in dependence on the ratio: distance z from the free glass surface versus corresponding critical radius R_c. The series of the s-shaped curves is drawn with parameter $\beta(z \to \infty)$ increasing from the uppermost curve to the lowest curve. (b) Nucleation activity ϕ of a planar interface in dependence on the wetting angle θ between the active substrate and the overgrowing cap-shaped nucleus.

work of nucleus formation ΔG_c is drastically reduced at $R_o/R_c \leq 10$. Here R_c is the radius of the critical cluster formed in a grain of radius R_o. With this second effect the nucleation catalysing effect of glass powder produced in glass milling and disintegration can be explained [4, 14, 25]. In a similar way it can be shown that in the case of bulk nucleation surface catalysis effects begin at a relative distance z/R_c from the free glass surface given by $0 \leq z/R_c \leq 1.5$ [4, 14, 25].

As an insert on the same figure (Fig. 2) the well known dependence of the nucleation activity ϕ of active heterogeneous foreign substrates on the wetting angle θ between the substrate and an overgrowing cap shaped nucleus (see e.g. [4, 27, 28]) is also given. In the heterogeneous catalysis case according to a general theorem formulated by Kaischew (see literature given in [4, 28]) the activity ϕ defined as $\phi = \Delta G_c^*/\Delta G_c^o$ is connected with the volume of the hetrogeneously and homogeneously formed nucleus via $\phi = V_c^*/V_c^o$. Here V_c^* and V_c^o are the volumes of nuclei formed heterogeneously and homogeneously, respectively.

The analogy of the ϕ vs. θ curve with the discussed $\Delta G_c(z)/\Delta G_c(z \rightarrow \infty)$ vs. z/R_c curves is evident (compare Fig. 2a with 2b). It the last case, however, the distance z from the free surface and not the wetting angle θ determines the catalyzing effect.

When a glass sample is heated from room temperature up to the crystallisation temperature, nucleation on the surface of the grains (or in glass dust and powders) begins even below T_g. Thus, at further heat treatment at temperatures $T > T_g$ crystallization of the sample begins from these previously formed nuclei, usually termed as athermal nuclei.

In analogy to this formalism in [14, 25, 29] the activity of the free glass surface or of surface defects is determined using as a starting point the presumption that nucleation is more probable, the less material of the matrix is elastically deformed (see also [4]). In this way (see Figs 3–5) the influence of edges, of grooves and of surface contaminants can be explained at least qualitatively. Such a finding is in accordance with experimental results obtained by Zanotto [17, 30] and Müller [16, 31] and with additional evidence summarized in [25]. According to the classical concepts of hetrogeneous nucleation [4, 28] the formation of a nucleus (e.g. in vapour condensation) is most probable in a groove: i.e. at a place where its volume is considerably reduced (see Fig. 3a). On edges or cones the formation of a condensate is inhibited. In nucleation on the surface of an elastic isotropic solid accounting for the influence of elastic energy, on the contrary, edges are most active (where nucleation is accompanied with minimal matrix deformation, see Fig. 3b and Fig. 3c). Thus, while heterogeneous nucleation begins in grooves and scratches, surface nucleation of an isotropic elastic solid (e.g. of a devitrifying glass) begins on its edges. In both cases a distorted surface is more active in respect to nucleation as discussed in details in [25] and as illustrated on Figs 3 and 4.

When active substrates (for example, heterogeneous foreign contaminants or glass dust) are spread on the surface, nucleation is initiated since the specific surface energy at the foreign substrate/crystal interface is lower

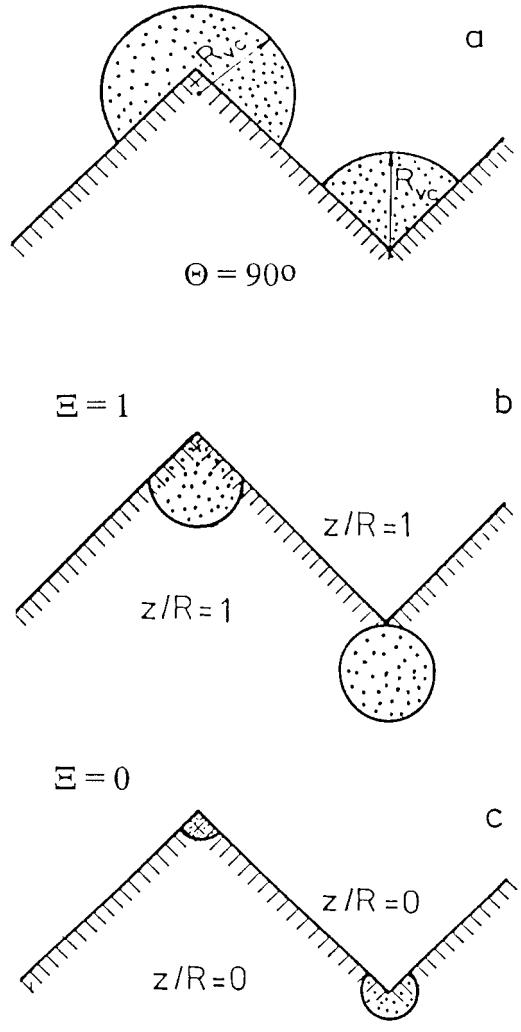

Figure 3 Different possibilities for the formation of new phase clusters in the case of a rough interface. (a) Vapour condensation on edges and grooves of a surface having activity $\theta = 90^\circ$ (no influence of strains). (b) and (c) Influence of elastic stains: surface induced crystallization on edges and grooves for $\Xi = 1$ and $\Xi = 0$, respectively.

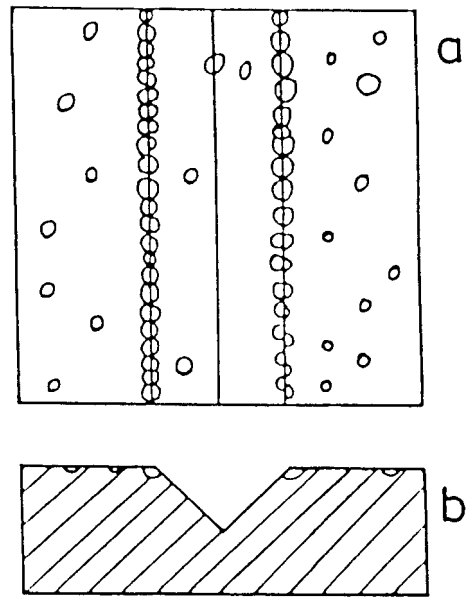

Figure 4 Preferred sites for the formation of crystalline clusters of the new phase accounting for the influence of elastic strains generated. Crystallization occurs along the edges of scratches and not in the grooves as should be expected in the case of heterogeneous nucleation. (a) Overview of the glass sample; (b) cross section of the same sample.

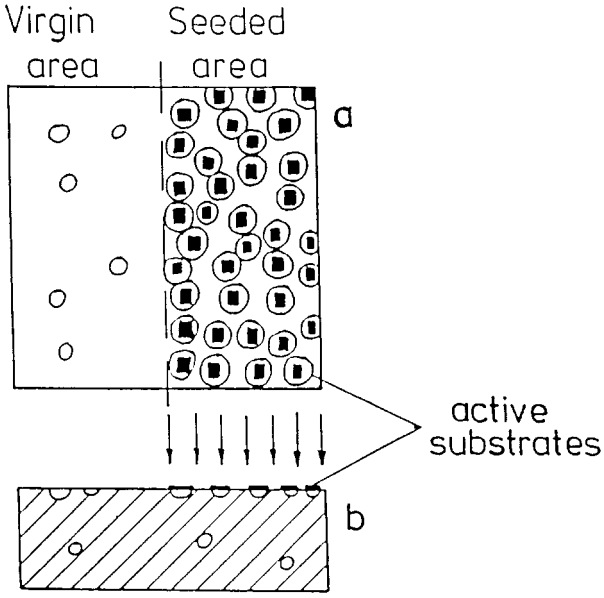

Figure 5 Glass surface seeded with active contaminants also induces nucleation. (a) Overview of the glass sample; (b) cross section of the same sample.

than that at crystal/air interface (see Fig. 5). Both effects have been experimentally observed (see [25]).

3. Kinetics of overall crystallization of grained glass

The kinetics of overall crystallization of grained glass representing an ensemble of equal spheres has been treated in details by Mampel [32] and Todes [33]. However, only numerical, non analytical solutions can be obtained in the general case analyzed by these authors. This is why, a simplified treatment of the problem is presented here for three particular cases. It is formulated in such a approximative way, that an analytical solution becomes possible.

According to Avrami's model [34] (see also [4, 35]) the fraction $\alpha(t)$ of crystallized volume changes with time t as

$$\mathrm{d}[\alpha(t)] = [1 - \alpha(t)]\,\mathrm{d}[Y(t)] \tag{6}$$

where $Y(t)$ is the so called extended volume.

After integration the well known result

$$\alpha(t) = 1 - \exp[-Y(t)] \tag{7}$$

is obtained.

In terms of the above mentioned general Avrami formulation to analyze particular models of crystallization is equivalent to assume different $Y(t)$ dependences.

Let us suppose that on the free surface of the grained glass sample exists a concentration of M^* athermal nuclei growing with a velocity ν. These athermal nuclei are formed at lower temperatures in the process of temperature rise, mainly under the catalytic effect of foreign substrates, dust, active sites etc. In the initial stages of crystallization when the growing crystallites do not

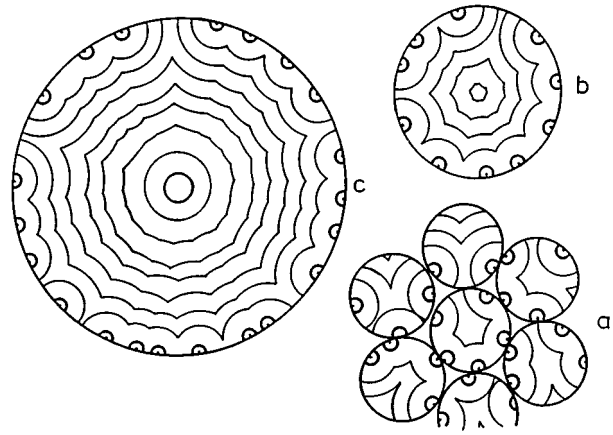

Figure 6 Change of mode and dimensionality of growth of athermal crystalline nuclei in glass grains with different grain radius R_o: (a) Small (dust-like) grains: three-dimensional growth, $n = 3$, (b) medium sized glass grains: $3 > n > 1$ and (c) large sized grains: $n \approx 1$ (schematically).

interact, yet (as illustrated in Fig. 6) three-dimensional growth is to be expected. Thus, at $t \to 0$

$$Y(t) = M^* S^* \nu^3 t^3 = M^*(3/R_o)(2\pi/3)\nu^3 t^3 \tag{8}$$

holds.

The surface area of a glass grain being $S_o = 4\pi R_o^2$ and the number of grains in a cm^3 of the sample being $N_o = 1/[(4\pi/3)R_o^3]$, it turns out that in the above formula the total surface area S^* of the grained probe can be expressed as

$$S^* = S_o N_o = 3/R_o.$$

Three-dimensional growth of the surface nucleated crystallization centres becomes practically impossible after the time t_3 has elapsed, where

$$t_3 = (1/2)/\sqrt{M^* \nu^2}. \tag{9}$$

The above derivation is obvious from Fig. 7 and taking into account that

$$d_o \approx 2\nu t_3 \tag{9-a}$$

$$M^* = 1/d_o^2. \tag{9-b}$$

Here d_o is the size up to which the athermal nuclei with a surface concentration M^* will grow up to the end of the three-dimensional growth stage. Moreover, from Fig. 6 one can see that for glass semolina samples for which the condition $(R_o/\nu) \to 0$ is fulfilled, the fraction $\alpha(t_3)$ crystallized after time t_3 is $\alpha(t_3) \approx 1$.

After an intermediate period of crystal selection, radial growth of a colony of needle like crystallites, perpendicular to the surface of the grains is usually observed (see Figs 6 and 7). In this third stage of the process

$$Y(t) = M^*(3/R_o)(\pi/4)d_o^2 \nu t \tag{10}$$

is to be expected. For this $Y(t)$-law, at $Y(t) \ll 1$ and $M^* d_o^2 = 1$, Equation 7 gives

$$\alpha(t) \cong (3/R_o)vt \tag{11}$$

i.e. the same approximative solution as this one following from the classical Jander law [36]

$$\alpha(t) = 1 - [1 - vt/R_o]^3 \cong (3/R_o)vt \tag{12}$$

for $(vt/R_o) \to 0$. Thus, from the preceding considerations it is to be expected that in dependence of the v/R_o ratio a change from

$$\alpha(t) = 1 - \exp\left(\left(-b_3 v^3 t^3\right)/R_o\right) \tag{13a}$$

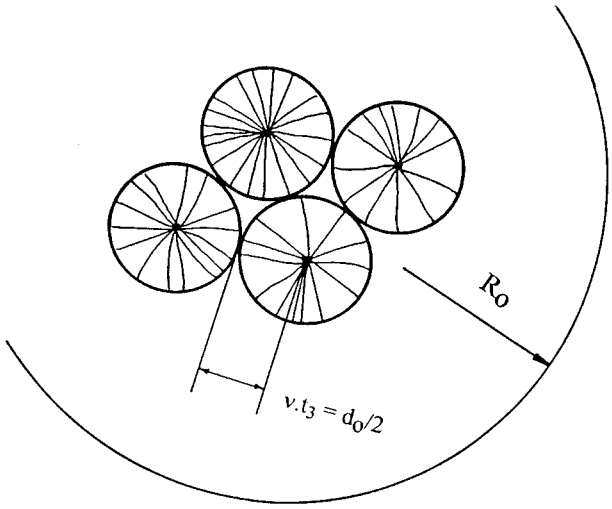

Figure 7 Illustrating the determination of the time t_3 (see Equations 9) during which athermal crystalline nuclei with concentration M^* on the surface of the glass grain grow as caps into the bulk of this grain. v, $d_o(t_3)$, and R_o denote the linear growth rate, the size of the caps and the grain radius, respectively.

to the dependence

$$\alpha(t) = 1 - \exp((-b_1 vt)/R_o) \tag{13b}$$

should be expected. Here, with b_3 and b_1, $b_3 = 3M^*(2\pi/3)$ and $b_1 = 3M^*(\pi/4)d_o^2$ are denoted.

It follows also from Equations 13 that at constant temperature and at one and the same time t_x the fractions $\alpha(t_x)$ which crystallize in glass semolina samples with different grain radii should give a straight line in co-ordinates $\log[1-\alpha(t_x)]$ vs. $1/R_o$ (or in co-ordinates $\alpha(t_x)$ vs. $1/R_o$ for small α values).

On Fig. 8a the results of a thorough investigation of the crystallization kinetics of different fractions of $NaPO_3$-glass semolina samples are given. Under the conditions of our experiment, from the water soluble $NaPO_3$ glass α-$NaPO_3$ crystalline phase with cyclic structure is formed which is also water soluble (see [4, 20, 37]. This gives the possibility to follow the $NaPO_3$ crystallization kinetics using not only density, X-ray or IR measurements but also simple analytical determinations (see [20]). The $\alpha(t)$ curves on Fig. 8a are obtained at different temperatures guaranteeing a nearly equal time of full crystallization for every fraction investigated.

On Fig. 8b data on the kinetics of overall crystallization of technical diopside precursor glass semolina samples are also presented [13].

On Fig. 9 the data from Fig. 8 are given in co-ordinates $\log[-\log(1-\alpha)]$ vs. $\log t$ according to Avrami's equation [34]. In these co-ordinates the $\alpha(t)$ data obtained for $NaPO_3$ glass semolina samples with different grain radii R_o give straight lines with an n value changing from $n = 2.6$ ($R_o < 0.04$ mm), $n = 2.5$ ($R_o = 0.05$–0.08 mm), $n = 1.7$ ($R_o = 0.2$–0.25 mm) to $n = 1.1$ ($R_o = 0.375$–0.5 mm). The same low n value ($n = 1.1$) as for the coarsest $NaPO_3$ glass fraction is also observed for the data obtained for diopside

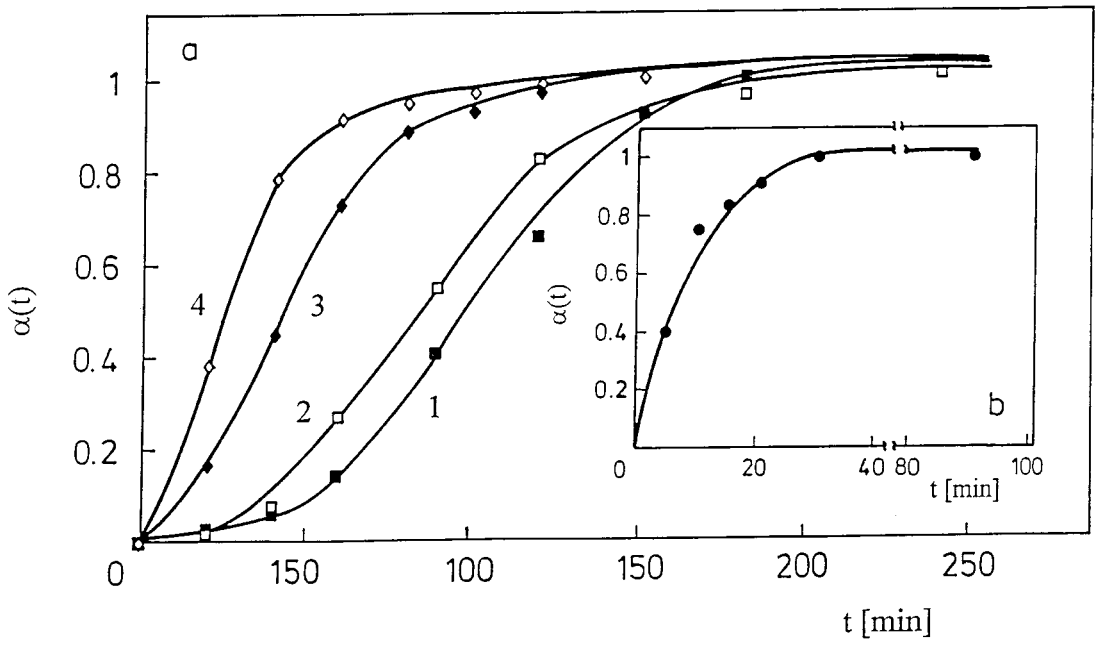

Figure 8 Overall crystallization kinetics of different fractions of glass semolina samples. (a) Overall crystallization of $NaPO_3$ glass semolina samples with different radii R_o and heat treated at different temperatures: curve 1 (■) 302 °C, $R_o < 0.04$ mm; curve 2 (□) 306 °C, $R_o = 0.05$–0.08 mm; curve 3 (♦) 325 °C, $R_o = 0.2$–0.25 mm; curve 4 (◇) 332 °C, $R_o = 0.375$–0.25 mm; (b) $\alpha(t)$ data obtained for the crystallization of diopside precursor glass heat treated at 1060 °C. $R_o = 1.25$ mm.

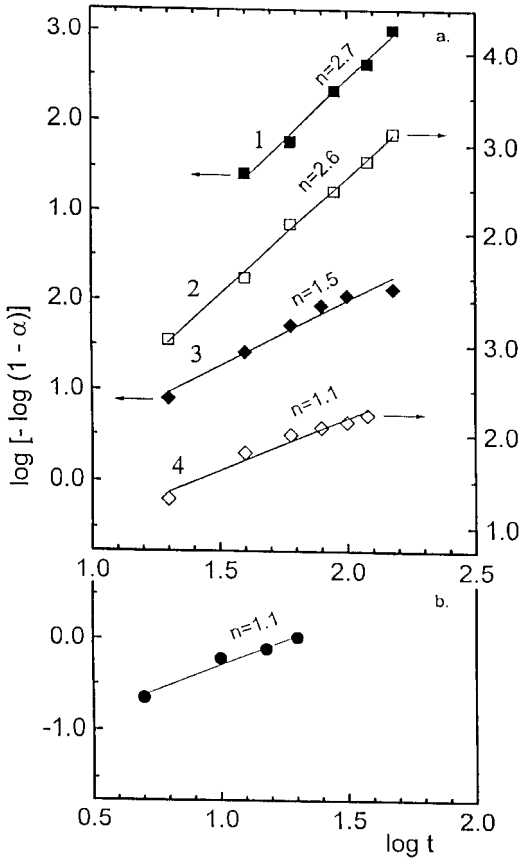

Figure 9 The $\alpha(t)$ data from Fig. 8a and b in Avrami coordinates: The numbers of the straight lines correspond to those of the $\alpha(t)$ curves given on Fig. 8 while the parameter to each straight line gives the value of the respective Avrami coefficient n.

glass semolina samples with a relatively great radius $R_o = 2.5$ mm (see Fig. 9b).

In the same co-ordinates we have also analyzed the results of Filipovich *et al.* [18] on overall crystallzation of cordierite glass semolina samples with different grain sizes ($R_o = 50$–80 μm and $R_o = 0.5$–2.5 μm). In correspondence with above derivations n changes from $n = 1, 5$ to $n = 2$ for the samples with larger and smaller grain sizes, respectively.

In the already cited paper [20] additional evidence for the change of n in the surface induced crystallization of a number of model glasses (for $ZnO{\cdot}PO_5$, $CdO{\cdot}P_2O_5$, $Li_2O{\cdot}P_2O_5$ etc.) is also summarized. There n changes also from $n \approx 3$–4 to 1–2 when going from smallest glass fractions to millimetre sized semolina samples.

On Fig. 10a and b data on overall crystallization of different fractions $NaPO_3$ glass semolina samples are presented in co-ordinates $\alpha(R_o)$ vs. R_o and $\alpha(R_o)$ vs. $1/R_o$, respectively. As seen, the expected $\alpha(R_o)$ dependence following from Equations 13 is fulfilled.

4. Kinetics of sintering

The sintering kinetics of glass grains and powders is usually described in terms of Frenkel's equation

$$\frac{d\Delta x}{x_o dt} = \frac{8\pi\sigma}{3\eta R_o} \tag{14}$$

where $\Delta x/x_o$ is the degree of relative sintering.

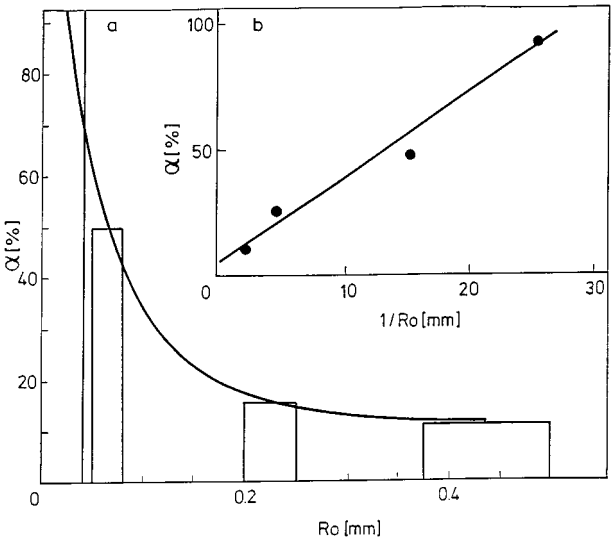

Figure 10 Overall crystallization of different fractions of $NaPO_3$ glass semolina samples at constant time of heat treatment (1.5 h) at 302 °C. (a) α data as a function of grain radius R_o; (b) the same data in coordinates α vs. $1/R_o$.

In 1989 Müller [16] proposed to connect sintering and crystallization kinetics as

$$\frac{d\Delta x}{x_o dt} = \frac{8\pi\sigma}{3\eta R_o}[1 - \alpha(t)]. \tag{15}$$

The idea behind this equation is that upon crystallization the contact between two sintering droplets, underlying Frenkel's model is diminished proportional to $\alpha(t)$, the fraction crystallized. Here a generalization of Müller's original model is attempted and a number of consequences following from it is derived.

First we introduce via

$$\frac{\sigma}{\eta R_o} = \frac{1}{\tau_o} \tag{16}$$

a characteristic time scale τ_o for the sintering process without crystallization. In a similar way using the results of the previous paragraphs we can also introduce via

$$\frac{1}{\tau_1} = M^* \frac{3}{R_o} \pi \left(\frac{d_o}{2}\right)^2 \nu \tag{17a}$$

$$\frac{1}{\tau_2} = \left(M^* \frac{3}{R_o} \pi \frac{d_o}{2} \nu^2\right)^{1/2} \tag{17b}$$

$$\frac{1}{\tau_3} = \left(M^* \frac{3}{R_o} \pi \frac{2}{3} \nu^3\right)^{1/3} \tag{17c}$$

three characteristic times, governing the crystallization process in an ensemble of sinter-crystallizing particles of radius R_o for the already discussed different cases of crystal growth (see Equations 13). In the case of linear growth of a colony of crystals using Equations (10–13) we have to write after integration of Equation 15 with the boundary condition

$$\frac{d\Delta x}{x_o} = 0 \qquad \text{at } t \to 0 \tag{18}$$

that

$$\frac{\mathrm{d}\Delta x}{x_o \mathrm{d}t} = \frac{8\pi\sigma}{3}\frac{\tau_1}{\tau_o}\left[1 - \exp\left(-\frac{t}{\tau_1}\right)\right]. \qquad (19)$$

Let us introduce with $I_1(t/\tau_1)$, $I_2(t/\tau_2)$ and $I_3(t/\tau_3)$ the integrals

$$I_1\left(\frac{t}{\tau_1}\right) = \int_0^{t/\tau_1} \exp\left(-\frac{t}{\tau_1}\right) \mathrm{d}\left(\frac{t}{\tau_1}\right) = \left[1 - \exp\left(-\frac{t}{\tau_1}\right)\right] \qquad (20a)$$

$$I_2\left(\frac{t}{\tau_2}\right) = \int_0^{t/\tau_2} \exp\left(-\frac{t}{\tau_2}\right)^2 \mathrm{d}\left(\frac{t}{\tau_2}\right) = \frac{\sqrt{\pi}}{2}\Phi\left(\frac{t}{\tau_2}\right) \qquad (20b)$$

$$I_3\left(\frac{t}{\tau_3}\right) = \int_0^{t/\tau_3} \exp\left(-\frac{t}{\tau_3}\right)^3 \mathrm{d}\left(\frac{t}{\tau_3}\right) \qquad (20c)$$

where $\Phi(t/\tau_2)$ in Equation 20b is the error integral. Thus, the final result for every one of the three cases considered can be written in the form

$$\frac{\Delta x}{x_o} = \frac{8\pi}{3}\frac{\tau_n}{\tau_o} I_n\left(\frac{t}{\tau_n}\right). \qquad (21)$$

In Fig. 11 the course of the above three integrals $I_n(t/\tau_n)$ is given in relative co-ordinates $I_n(t/\tau_n)/I_n(\infty/\tau_n)$ vs. the time t/τ_n where $I_n(\infty/\tau_n)$ denotes the value of the integral $I_n(t/\tau_n)$ in the interval $(0, \infty)$.

For any of the above integrals an approximative solution can be also written after a truncated Taylor expansion of the integrand. Thus, confining ourselves to the second member of the expansion we have for $t/\tau_n < 1$

$$I_1 \approx I_1^* = \frac{t}{\tau_1}\left[1 - \frac{1}{2}\left(\frac{t}{\tau_1}\right)\right] \qquad (22a)$$

$$I_2 \approx I_2^* = \frac{t}{\tau_2}\left[1 - \frac{1}{3}\left(\frac{t}{\tau_2}\right)^2\right] \qquad (22b)$$

$$I_3 \approx I_3^* = \frac{t}{\tau_3}\left[1 - \frac{1}{4}\left(\frac{t}{\tau_3}\right)^3\right]. \qquad (22c)$$

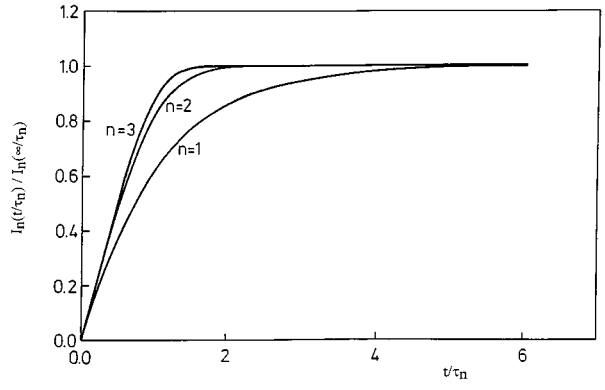

Figure 11 Time evolution of the integrals $I_n(t/\tau_n)$ (Equations 20a–20c) in relative coordinates $I_n(t/\tau_n)/I_n\,(\infty/\tau_n)$ vs. t/τ_n.

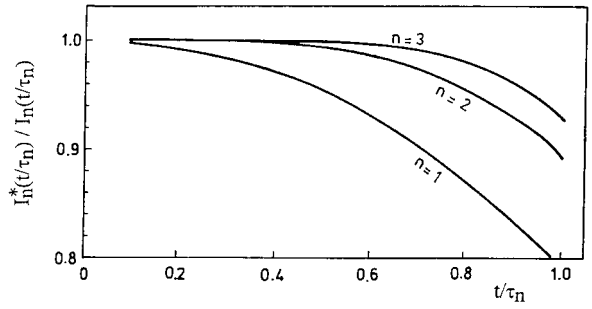

Figure 12 Demonstration of the applicability of the approximations $I_n^*(t/\tau_n)$ given by Equations 22a–22c by presenting in coordinates $I_n^*(t/\tau_n)/I_n(t/\tau_n)$ vs. t/τ_n.

In Fig. 12 the applicability of the approximations $I_n^*(t/\tau_n)$ (Equations 22a–22c) is illustrated by presenting these approximations in relative co-ordinates $I_n^*(t/\tau_n)/I_n(t/\tau_n)$ vs. t/τ_n. It is seen that the higher n the more correct the respective approximation is.

In this way it turns out that for the initial stages of crystallization (i.e. for $t/\tau_n < 1$) we can write in all the three cases considered

$$\frac{\Delta x}{x_o} \approx \frac{8\pi}{3}\frac{t}{\tau_o}\left[1 - \frac{1}{n+1}\left(\frac{t}{\tau_n}\right)^n\right] \qquad (22d)$$

where $n = 1$, $n = 2$ or $n = 3$, respectively.

The concrete choice of any of the above equations depends on the crystallisation morphology which is not known in advance. In making the respective decision here direct microscopic observations should be of importance. In line with the discussion in the preceding section they could allow to choose the correct n value. Thus, if needle-like growth and well defined crystallization fronts are observed, $n = 1$ should be chosen etc.

More complicated is the case when η (or in an equivalent formulation the time τ_o) depends on the degree of crystallization. The simplest possible assumption which could be made in this case is that η increases in a way similar to the viscosity increase of a suspension. For the classical case of a diluted suspension the Einstein formula reads

$$\eta = \eta_o(1 + a_o C) \qquad (23)$$

Here C is the volume concentration of the suspension and a_o is a well known constant ($a_o = 2.5$).

For the more complicated case of viscous flow of concentrated polymer solutions different formulae are proposed in the literature [39] which can be written as

$$\eta = \eta_o\left(1 + a_o^* C^n\right). \qquad (24)$$

In an analogy of such a formula we could expect in a first approximation that

$$\eta = \eta_o\left\{1 + B_o[\alpha(t)]^u\right\} \qquad (25)$$

where B_o and u are constants.

Thus, Equation 15 could be transformed into

$$\frac{\mathrm{d}\Delta x}{x_o \mathrm{d}t} = \frac{8\pi}{3}\frac{\alpha}{R_o}\frac{1}{\eta_o\left\{1 + B_o[\alpha(t)]^u\right\}}[1 - \alpha(t)]. \qquad (26)$$

In this way it turns out that for the initial stages of sinter-crystallization i.e. for $t/\tau_n \to 0$

$$\frac{\mathrm{d}\Delta x}{x_0 \mathrm{d}t} \approx \frac{8\pi}{3}\frac{t}{\tau_0}. \qquad (27)$$

In the literature experimental data can be found on the kinetics of sintering for various glass forming systems [16, 18]. They will be analyzed in terms of the above derived formalism in a following investigation.

5. Discussion and conclusions

The above derived formalism gives a new possibility to consider and predict both the kinetics of crystallization and of sintering in sinter crystallization experiments. In the present investigation a simple approximative way is given in order to derive analytical expressions describing both processes. Crystallization influences sintering and the above discussed model of Müller and its generalization made here gives a way for quantitative analysis of the sintering kinetics. It is assumed here (and confirmed by experiment) that crystallization begins together with the process of sintering on the free glass surfaces. We have mentioned several experimental investigations in which the kinetics of overall crystalization is investigated. The results given there seem to be in accordance with the prediction of the formalism developed here.

We hope that the present analysis could initiate further investigations on sinter crystallization and especially on sintering kinetics of technically important glasses. It can be shown that the strength of glass ceramic materials obtained by sinter crystallization is essentially determined by the process of sintering itself [13]. The way and mechanism of crystallization determines on the other hand the general appearance of samples and thus the possibility for their utilization (e.g. the marble like resemblance of glass ceramics for architectonic purposes [13, 21]).

There are, however, very few examinations of the formation process and especially on the influence of the kinetics of crystallization and of sintering on the properties of the technical glass ceramic materials formed in this way.

Acknowledgements

The authors gratefully acknowledge the financial assistance of the Deutsche Forschungsgemeinschaft and of the Bulgarian National Scientific Fund under Contract X 622.

References

1. P. W. MCMILLAN, "Glass-Ceramics" (Academic Press, London, 1964).
2. Z. STRNAD, "Glass-Ceramic Materials" (Elsevier, Amsterdam, 1986).
3. A. I. BEREJNOI, "Sitalli i Fotositalli" (Mashinostroene, Moscow, 1981).
4. I. GUTZOW and J. SCHMELZER, "The Vitreous State" (Springer, Berlin, New York, 1995).
5. I. GUTZOW, *Contemp. Phys.* **21** (1980) 121, 243.
6. R. de REAUMURQ, Memoires I'Academie Royale des Sciences, (Paris, 1739).
7. G. TAMMANN, "Der Glaszustand" (Leopold Voss Verlag, Leipzig, 1933).
8. B. Y. BLUMBERG, "Introduction into the Physical Chemistry of Glasses" (Chemistry State Publishers, Leningrad, 1939).
9. W. NACHTIGAL, V. OPITZ, E. PECH and H. J. POHL, "Glas" (Verlag der Wissenschaft, Berlin 1988).
10. W. SACK, in "Beiträge zur Angewandten Glasforschung," edited by E. Schott (Universität Mainz, 1959) p. 111.
11. M. TASHIRO, *J. Non-Cryst. Sol.* **73** (1985) 575.
12. E. M. RABINOVICH, in "Nucleation and Crystallization in Glasses," Vol. 4, edited by J. H. Simons, D. R. Uhlmann and G. H. Bell (American Ceram. Soc., Westerville, 1982) pp. 327–333.
13. A. KARAMANOV, I. GUTZOW, I. PENKOV, J. ANDREEV and B. BOGDANOV, *Glastech. Ber. Glass Sci. Technol.* **67** (1994) 202.
14. J. SCHMELZER, R. PASCOVA, J. MÖLLER and I. GUTZOW, *J. Non-Cryst. Sol.* **162** (1993) 26.
15. R. MÜLLER, TH. HUBERT and M. KIRSCH, *Silikattechnik* **37** (1986) 111.
16. R. MÜLLER, D. THAMM, in Proceedings 4th Otto-Schott Kolloquium, Wissenschaftliche Zeitschrift der Iniversität Jena, 1990, p. 187.
17. E. D. ZANOTTO, *J. Non-Cryst. Sol.* **129** (1991) 183.
18. A. M. KALININA, V. N. FILIPOVICH and Z. D. ALEKSEEVA, *Fiz. Khim. Stekla* **18** (1992) 52.
19. V. N. FILIPOVICH, Z. D. ALEKSEEVA and A. M. KALININA, *ibid* **16** (1990) 81.
20. I. GUTZOW, *J. Cryst. Growth* **48** (1979) 569.
21. A. KARAMANOV, I. GUTZOW, B. BOGDANOV, I. CHOMAKOV and A. KOSTOV, *Glastech. Ber. Glass Sci. Technol.* **67** (1994) 227.
22. A. R. BOCCACCINI, M. KOPF and W. STUMPFE, *Ceramics International*, in print.
23. K. J. THOME-KOZMIENSKY, in "Thermische Abfallbehandlung," edited by U. Pahl and C. Gammelin (EF-Verlag fur Energie und Umwelttechnik GMBH) 1996.
24. K. TABATA, *J. Amer. Ceram. Soc.* **10** (1927) 6.
25. J. SCHMELZER, J. MÖLLER, I. GUTZOW, R. PASCOVA, R. MÜLLER and W. PANNHORST, *J. Non-Cryst. Sol.* **183** (1995) 215.
26. F. R. N. NABARRO, *Proc. Royal Soc.* (London) **A 175** (1940) 519.
27. J. P. HIRTH, G. M. POUND, "Condensation and Evaporation" (Pergamon Press, London, 1963).
28. B. MUTAFCHIEV, in "Handbook of Crystal Growth," edited by T. D. J. Hurle (Elsevier Science Publishers, Amsterdam 1993) p. 187.
29. J. MÖLLER, J. SCHMELZER, I. GUTZOW and R. PASCOVA, *Phys. Stat. Sol. (b)* **180** (1993) 315.
30. E. D. ZANOTTO, *J. Non-Cryst. Sol.* **129** (1991) 183.
31. R. MÜLLER, R. NAUMANN and S. REINSCH, in Proc. Bunsengesellschaft on Phys. Chem. Glasses, March 1996, Jena, in print.
32. K. MAMPEL, *Z. Phys. Chem.* **A 187** (1940) 43, 225.
33. K. M. TODES, *Zh. Fiz. Khim. (USSR)* **14** (1940) 1224.
34. M. AVRAMI, *J. Chem. Phys.* **7** (1939) 1103; **8** (1940) 212; **9** (1941) 177.
35. I. GUTZOW, D. KASHCHIEV and I. AVRAMOV, *J. Non-Cryst. Sol.* **73** (1985) 477.
36. P. BARRET, "Cinetique Heterogene" (Gauthier-Villars, Paris 1973) Chap. 5.
37. I. GUTZOW, *Z.Anorgan.Allgemeine Chemie* **302** (1959) 18, 259.
38. R. MÜLLER, D. THAMM and M. KIRSCH, in Proc. SILICER, 1990, Nürnberg.
39. S. MIDDLEMANN "The Flow of High Polymers" (Academic Press, New York, 1962) Chap. 4.

Received 18 November 1996
and accepted 15 September 1998